EFFECTS OF STENOSIS AND DILATATION ON FLOW OF BLOOD MIXED WITH SUSPENDED NANOPARTICLES: A STUDY USING HOMOTOPY TECHNIQUE

T. Sudha
Department of Mathematics, Malla Reddy College of Engineering for Women,
Hyderabad, Telangana, INDIA

C. Umadevi
Department of Mathematics, T.K.R. College of Engineering and Technology
Hyderabad 500097, Telangana, INDIA

M. Dhange[*]
Department of Mathematics, B.L.D.E.A's V.P. Dr. P.G. Halakatti College
of Engineering and Technology, Vijayapur 586103, Karnataka, INDIA
E-mail: math.mallinath@bldeacet.ac.in

S. Manna
Discipline of Mathematics, Indian Institute of Technology, Indore-453552, Madya-Pradesh, INDIA

J. C. Misra
Indian Institute of Engineering Science and Technology, Shibpur, West Bengal, INDIA

The paper deals with a theoretical study on blood flow in a stenosed segment of an artery, when blood is mixed with nano-particles. Blood is treated here as a couple stress fluid. Stenosis is known to impede blood flow and to be the cause of different cardiac diseases. Since the arterial wall is weakened due to arterial stenosis, it may lead to dilatation /aneurysm. The homotopy perturbation technique is employed to determine the solution to the problem for the case of mild stenosis. Analytical expressions for velocity, shear stress at the wall, pressure drop, and flow resistance are derived. The impact of different physical constants on the wall shear stress and impedance of the fluid is examined by numerical simulation. Streamline patterns of the nanofluid are investigated for different situations.

Key words: stenosis, dilatation, couple stress fluid, impedance, shear stress.

MSC CLASSIFICATION: 74F05, 76A05, 76Z05, 82D80

1. Introduction

Arterial stenosis refers to the narrowing of a segment of an artery owing to the development of the arteriosclerotic deposition or different sorts of anomalous tissue development in the lumen of an artery, and as a result of this blood flow in the artery is impeded. In the course of time, this impediment of blood flow may harm the endothelial cells of the wall and may prompt further development of the stenosis. In this way, there is a coupling within the development of the flow of blood and stenosis in the artery since each

---

[*] To whom correspondence should be addressed

influences the other. The advancement of stenosis in an artery can have genuine outcomes and can disturb the normal working of the circulatory system.

Investigation of blood flow through stenosed blood vessels is one of the principal territories of research since in more than 30% cases of all deaths arise out of circulatory disorders. The circulatory irregularities may be manifested in the form of pain in the chest. Subsequently, there is a risk of death, if there is a sufficient reduction of blood supply to the brain. The large and medium-sized arteries are exceptionally flexible; exposing these arteries to high pressure makes them rigid as in the case of tubes. This change in property from flexibility to rigidity is called arteriosclerosis. The same thing happens with arterioles and small arteries wherein the arterial walls lose flexibility over a period of time.

One of the main reasons for circularity disorders is the development of stenosis in the arterial lumen. Stenosis can alter the normal functioning of the cardiovascular system. It increases the impedance to blood flow, resulting in enhanced blood pressure and tissue damage leading to dilatation of the stenosis. In this way, the total data of the streams in the conduits having stenosis and dilatation can provide better information on the condition of the streams in the physiological structure. Stenosis was first studied by Young [1], who made an observation that even mild stenosis can lead to measurable obstructions. This study was followed by a series of experimental/theoretical studies to measure the stream structures of blood flowing in vessels with mild narrowing by considering blood as Newtonian/non-Newtonian fluids under diverse circumstances [2-5].

Nowadays, nanotechnology has been significantly contributing to pharmaceutical material research. Nanoparticles are used to deliver the drug at the location of interest. The side effects of the medication can be reduced by adopting this procedure. In particular, nanoparticles are extensively used for the treatment of brain tumors, cleaning water, etc. The challenges associated with nanoparticle applications are to increase the amount of the drug carried by decreasing the size. The drug supply to the targeted organs can be achieved without the need of incomplete healing through the drug-coated balloon therapy. The drug reaches the targeted organ through the diffusion procedure and will affect the targeted region only. In this way, the side effects of the drug can be minimized effectively. Ramana *et al.* [6] described a method to of medicine delivery mechanism to the organ of interest by a medicine coated with nanoparticles. These new methods can influence the way drugs can be administered resulting in better health condition. Nadeem *et al.* [7] and Prasad *et al.* [8] investigated the Prandtl fluid model and couple stress fluid model in the existence of nanoparticle with stenosis.

The concentration scattering in a non-Newtonian liquid was studied by Jyotirmoy and Murthy [9], by considering different models like Carreau-Yasuda, Carreau, and Casson fluid. They evaluated the workable transport coefficients, i.e. convection, barter, and dispersion coefficients. Later, Elnaqeeb *et al.* [10] studied the flow through asymmetric stenosis and reported the impact of nanoparticle volume fraction on the blood flow dynamics. In their model they considered the classical viscous fluid to represent blood as a base fluid. Some researchers studied blood flow experimentally and concluded that blood dynamics is unlike a classical viscous fluid and the strong deviation in the flow is due to the presence of neutrally afloat blood components. Therefore, blood has a non-Newtonian structure and the stress tensor is used to construct the related constitutive equation.

The hemodynamic properties are mainly affected by blood components. The change in the radius of gyration is used to incorporate the deformation of the particles in the couple stress fluid model. The model of the couple stress fluid reasonably resembles blood flow as reported by Valanis and Sun [11]. Srinivasacharya and Srikanth [12], Ponalagusamy [13], and Reddy *et al.* [14] highlighted various effects of mild stenosis on fluid flow through a constriction. In these papers, the authors presented a theoretical study on blood as a couple stress fluid in a stenosed segment of an artery. However, it is noted that the concentration and temperature scattering in the considered domain in the presence of the catheter in case of couple stress fluid have not been given much attention.

As it is not possible to find out the closed-form solutions to the highly non-linear and coupled equations, the authors came with a highly interesting way to find out the asymptotic series solutions based on the perturbation methods. Wang *et al.* [15] studied the concentration transport in the straight uniformly packed porous media in order to understand the Taylor diffusion by series solutions. Nevertheless, the

perturbation methods have their own limitations, like considering the small parameter from the modeled equations which may not be always possible. Therefore, recently numerous new methods have been proposed without the necessity of considering the small parameter ([16, 17]). Among these, the Homotopy Perturbation Method (HPM) is prime wherein the intent is to capture the asymptotic form of a infinite series solution which is convergent. The HPM method is proposed by He [18]. In this method, a homotopy is found out based on the externally imposed parameter q. Several researchers [19-22] studied the nanoparticle suspended blood flow and showed that this technique will enable us to get appropriate results when these kinds of problems are modeled. The advancement of stenosis in an artery can have genuine outcomes and disturb the typical working of the circulatory system. Specifically, it might prompt: increased resistance to flow with a possible serious decrease in blood flow, increased risk of complete occlusion, abnormal cell development in the region of the stenosis, which builds the intensity of the stenosis, and tissue harm prompting post stenosis dilatation [23,24]. The authors investigated the influence of multiple stenoses and dilatation followed by stenosis on non-Newtonian fluid flow in stenosed arteries.

With the above inspiration, in this manuscript, blood flow is modeled as a flow of couple stress nanofluid flow, by considering the arterial segment to be of an irregular geometry (cf. Fig.1.). The HPM method with mild stenosis approximation has been used to deal with the modeled system. The pressure droplet, flow resistance, and shear-stress at the wall are analyzed and the influence of many important factors are illustrated graphically. The mathematical model is formulated and analyzed in Section 2. Computational results are discussed in Section 3.

2. Formulation of the problem and its solution

Let us consider the flow of blood as an incompressible couple stress fluid through an axisymmetric artery (tube) having stenosis, which transforms to a dilatation at a later stage (Fig.1).
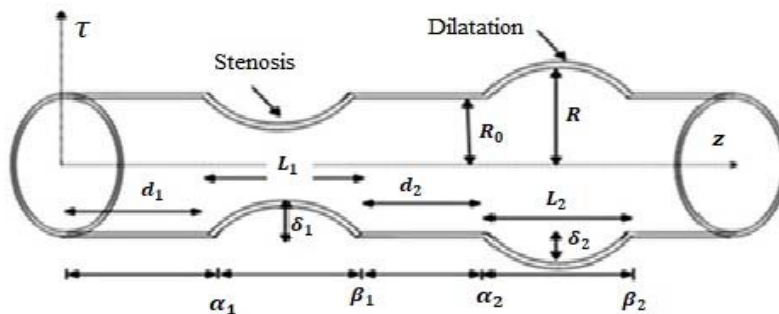

Fig.1. Schematic graph of the tube with stenosis and dilatation.

The geometry of the wall having stenosis/dilatation can be described as [24]

$$h = \frac{R(z)}{R_0} = \begin{cases} 1 - \dfrac{\delta_i}{2R_0}\left[1 + \cos\dfrac{2\pi}{L_i}\left(z - \alpha_i - \dfrac{L_i}{2}\right)\right] & : \alpha_i \leq z \leq \beta_i, \\ \\ 1 & : \text{otherwise} \end{cases} \tag{2.1}$$

where δ_i stands for the ith abnormal section maximal distance which projects into the lumen and δ_1 represents stenosis and δ_2 represents aneurysms. R is the tube radius at dilatation, R_0 is the radius of the normal segment of the artery, L_i the length of ith diseased section length.

The distance of the origin from the first i^{th} diseased segment may be written as:

$$\alpha_i = \sum_{j=1}^{i}(d_j + L_j) - L_i \ .$$

(2.2)

The distance of the origin from the terminal of the ith abnormal segment is given by:

$$\beta_i = \sum_{j=1}^{i}\left(d_j + L_j\right)$$

(2.3)

where d_i denotes the space of the initial i^{th} diseased part and end of the $(i-1)^{th}$ abnormal segment or as of the beginning part when $i = 1$.

The scaling variables are stated as:

$$\bar{z} = \frac{z}{B}, \quad \bar{d}_1 = \frac{d_1}{B}, \quad \bar{L}_1 = \frac{L_1}{B}, \quad \bar{L}_2 = \frac{L_2}{B}, \quad \bar{B}_1 = \frac{B_1}{B}, \quad \bar{v} = \frac{B}{\delta U}v, \quad \bar{u} = \frac{u}{U},$$

$$\bar{R}(z) = \frac{R(z)}{R_0}, \quad \bar{\delta}_i = \frac{\delta_i}{R_0}, \quad \theta_t = \frac{T - \bar{T}_0}{\bar{T}_0}, \quad \sigma = \frac{\left(C - \bar{C}_0\right)}{\bar{C}_0}, \quad \bar{P} = \frac{P}{\mu U L / R_0^2},$$

$$\bar{q} = \frac{q}{\pi R_0^2 U}, \quad N_b = \frac{(\rho C)_P D_{\bar{B}} \bar{C}_0}{(\rho C)_f}, \quad N_t = \frac{(\rho C)_P D_T \bar{T}_0}{(\rho C)_f \beta},$$

$$G_r = \frac{g\beta \bar{T}_0 R_0^3}{\gamma^2}, \quad B_r = \frac{g\beta \bar{C}_0 R_0^3}{\gamma^2}, \quad \bar{\alpha} = a\alpha = \sqrt{\frac{\mu}{\eta}}a, \quad \bar{h} = \frac{h}{h_0}.$$

The key conditions for the flow of an incompressible couple stress fluid with suspended nanoparticles under the assumption of mild stenosis may be expressed as:

$$\frac{1}{r}\frac{\partial}{\partial r}\left(r\frac{\partial}{\partial r}\left(1 - \frac{1}{\bar{\alpha}^2}\nabla^2\right)u\right) = \frac{dp}{dz} + G_r\theta_t + B_r\sigma \ ,$$

(2.4)

$$0 = \frac{1}{r}\frac{\partial}{\partial r}\left(r\frac{\partial \theta_t}{\partial r}\right) + N_b\frac{\partial \sigma}{\partial r}\frac{\partial \theta_t}{\partial r} + N_t\left(\frac{\partial \theta_t}{\partial r}\right)^2 ,$$

(2.5)

$$0 = \frac{1}{r}\frac{\partial}{\partial r}\left(r\frac{\partial \sigma}{\partial r}\right) + \frac{N_t}{N_b}\left(\frac{1}{r}\frac{\partial}{\partial r}\left(r\frac{\partial \theta_t}{\partial r}\right)\right).$$

(2.6)

In the above, $\bar{\alpha}^2 = \dfrac{\mu}{\eta} a^2$ is the couple stress fluid parameter, $\sqrt{\mu/\eta}$ is a characteristic measure of the polarity of the liquid model, $\bar{\alpha}$ is the ratio of the artery to the material characteristic length $\sqrt{\mu/\eta}$ In the limiting case (as $\eta \to 0$ i.e $\bar{\alpha} \to \infty$), Eq.(2.4) converts to the equation of Navier-Stokes.

The limitations of the boundary conditions are well-defined as:

$$\frac{\partial u}{\partial r} = 0, \frac{\partial \theta_t}{\partial r} = 0, \frac{\partial \sigma}{\partial r} = 0 \ \ at \ r = 0, \tag{2.7}$$

$$u = 0, \ \theta_t = 0, \ \sigma = 0 \ at \ r = h(z), \tag{2.8}$$

$$\frac{\partial^2 u}{\partial r^2} - \frac{\eta}{r} \frac{\partial u}{\partial r} = 0 \ at \ r = h(z), \tag{2.9}$$

$$\frac{\partial^2 u}{\partial r^2} - \frac{\eta}{r} \frac{\partial u}{\partial r} \text{is finite } at \ r = 0. \tag{2.10}$$

The primitive of the coupled Eqs (2.5) and (2.6) of the model along with stated limitations of boundary conditions have been determined by employing the Homotopy Perturbation technique [18] and is given below as:

$$H(q_t, \theta_t) = (1 - q_t)\left[L(\theta_t) - L(\theta_{t10}) \right] + q_t \left[L(\theta_t) + N_b \frac{\partial \sigma}{\partial r} \frac{\partial \theta_t}{\partial r} + N_t \left(\frac{\partial \theta_t}{\partial r} \right)^2 \right], \tag{2.11}$$

$$H(q_t, \sigma) = (1 - q_t)\left[L(\sigma) - L(\sigma_{10}) \right] + q_t \left[L(\sigma) + \frac{N_t}{N_b} \left(\frac{1}{r} \frac{\partial}{\partial r} \left(r \frac{\partial \theta_t}{\partial r} \right) \right) \right] \tag{2.12}$$

where q_t is the embedding constant, which lies in the interval $0 \le q_t \le 1$.
For the sake of tractability, let us consider the linear operator

$$L = \frac{1}{r} \frac{\partial}{\partial r} \left(r \frac{\partial}{\partial r} \right).$$

The primary estimates σ_{10} and θ_{t10} are given by:

$$\sigma_{10}(r, z) = -\left(\frac{r^2 - h^2}{4} \right), \quad \theta_{t10}(r, z) = \left(\frac{r^2 - h^2}{4} \right). \tag{2.13}$$

Nano-particle phenomena and the temperature can be specified at $q_t = 1$ as:

$$(N_b - N_t)\left(\frac{r^4 - h^4}{64} \right) = \theta_t(r, z), \tag{2.14}$$

$$-\left(\frac{r^2-h^2}{4}\right)\frac{N_t}{N_b}=\sigma(r,z)\,.$$ (2.15)

The velocity of a fluid with nano-particle suspension is calculated from Eqs (2.4), (2.14), (2.15) and the boundary conditions stated above, and is expressed as:

$$u(r,z)=AI_0(\bar{\alpha}r)+\frac{r^6T}{2304}+\frac{r^4}{64}\left(\frac{T}{\bar{\alpha}^2}-S\right)+\frac{r^2}{4}\left(\frac{T}{\bar{\alpha}^4}-\frac{Th^4}{64}+\frac{h^2S}{4}-\frac{S}{\bar{\alpha}^2}\right)+$$

$$+T\left(\frac{1}{\bar{\alpha}^6}-\frac{h^4}{64\bar{\alpha}^2}\right)+S\left(\frac{h^2}{4\bar{\alpha}^2}-\frac{1}{\bar{\alpha}^4}\right)+\left(\frac{dp}{dz}\right)\left(\frac{r^2}{4}+\frac{1}{\bar{\alpha}^2}\right)-d\bar{\alpha}^2$$ (2.16)

where $T=G_r(N_b-N_t)$, $S=B_r\left(\frac{N_t}{N_b}\right)$ and

$$A=\frac{\left[\frac{h(\eta-1)}{2}\left(\frac{dp}{dz}+\frac{T}{\bar{\alpha}^4}-\frac{Th^4}{64}+\frac{h^2S}{4}-\frac{S}{\bar{\alpha}^2}\right)+(\eta-5)\frac{Th^5}{384}+\frac{h^3}{16}(\eta-3)\left(\frac{T}{\bar{\alpha}^2}-S\right)\right]}{h\bar{\alpha}^2I_0(\bar{\alpha}h)-\bar{\alpha}I_1(\bar{\alpha}h)-\eta\bar{\alpha}I_1(\bar{\alpha}h)}\,,$$

$$d=1/\bar{\alpha}^2\left[AI_0(\bar{\alpha}h)+\frac{h^6T}{2304}+\frac{h^4}{64}\left(\frac{T}{\bar{\alpha}^2}-S\right)+\frac{h^2}{4}\left(\frac{T}{\bar{\alpha}^4}-\frac{Th^4}{64}+\frac{h^2S}{4}-\frac{S}{\bar{\alpha}^2}\right)+\right.$$

$$\left.+T\left(\frac{1}{\bar{\alpha}^6}-\frac{h^4}{64\bar{\alpha}^2}\right)+S\left(\frac{h^2}{4\bar{\alpha}^2}-\frac{1}{\bar{\alpha}^4}\right)+\left(\frac{dp}{dz}\right)\left(\frac{h^2}{4}+\frac{1}{\bar{\alpha}^2}\right)\right].$$

Some of the important dimensional physical quantities are presented below. The flow rate q is given by

$$q=\int_0^h 2ru\,dr.$$ (2.17)

Upon substituting Eq.(2.16) into Eq.(2.17), the flow rate is expressed as:

$$q=A\left(\frac{2h}{\bar{\alpha}}I_1(\bar{\alpha}h)-h^2I_0(\bar{\alpha}h)\right)-\frac{h^4}{8}\left(\frac{dp}{dz}\right)-\frac{Th^8}{3072}+$$

$$-\frac{h^6}{96}\left(\frac{T}{\bar{\alpha}^2}-S\right)-\frac{h^4}{8}\left(\frac{T}{\bar{\alpha}^4}-\frac{Th^4}{64}+\frac{h^2S}{4}-\frac{S}{\bar{\alpha}^2}\right).$$ (2.18)

From Eq.(18), the expression for the pressure gradient is obtained as:

$$\frac{dp}{dz} = \frac{8q}{Mh^4} + \frac{T}{M}\left[\frac{h^4}{384} - \frac{hD(\eta-5)}{48K}\right] - \left[\frac{T}{\bar{\alpha}^4} - \frac{Th^4}{64} + \frac{h^2S}{4} - \frac{S}{\bar{\alpha}^2}\right] + \\ + \frac{1}{M}\left[\left(\frac{T}{\bar{\alpha}^2} - S\right)\left(\frac{h^2}{12} - \frac{D(\eta-3)}{2Kh}\right)\right] \quad (2.19)$$

where

$$K = h\bar{\alpha}^2 I_0(\bar{\alpha}h) - \bar{\alpha}I_1(\bar{\alpha}h) - \eta\bar{\alpha}I_1(\bar{\alpha}h),$$

$$D = \frac{2h}{\bar{\alpha}}I_1(\bar{\alpha}h) - h^2 I_0(\bar{\alpha}h), \qquad M = \frac{4D(\eta-1)}{Kh^3} - 1.$$

The pressure drop over one wavelength $p(0) - p(\lambda)$ is given by:

$$\Delta p = -\int_0^1 \frac{dp}{dz} dz. \quad (2.20)$$

The impedance is denoted by λ and is defined by

$$\lambda = \frac{\Delta p}{q}. \quad (2.21)$$

The pressure drop in the normal portion of the artery, $h = 1$ is given by

$$\Delta p_n = \left[-\int_0^1 \frac{dp}{dz} dz\right]_{h=1.} \quad (2.22)$$

The flow resistance directly impacts the stream of blood and has a direct connection with the flow rate of blood. The impedance within the normal artery may be computed as:

$$\lambda_n = \frac{\Delta p_n}{q}. \quad (2.23)$$

The normalized impedance can be calculated as:

$$\bar{\lambda} = \frac{\lambda}{\lambda_n}. \quad (2.24)$$

The shear stress in blood vessel walls is one of the physical quantities which have a significant influence on the flow of fluid at the wall. The wall shear-stress may be computed by using the formula:

$$\tau_h = -\frac{h}{2}\frac{dp}{dz}. \quad (2.25)$$

3. Computational results and discussion

In order to illustrate the applicability of the analytical study presented above, appropriate numerical computation has been made by considering the specific values of the different parametric constants. The numerical results are presented graphically. The effects of stenosis, dilatation, the radius of the tube, the length of the arterial segment length of the stenosis/dilatation, involved in the study on different physical variables have been examined. Values of impedance $\left(\bar{\lambda}\right)$ and wall shear stress $\left(\tau_h\right)$ have been computed for different values of the parameters with the help of *MATHEMATICA* software and all the numerical results are presented graphically in Figs 2-19. It may be noted that Figs. 2-11 are plotted for examining the variation impedance $\left(\bar{\lambda}\right)$ with stenosis/dilatation parameters.

Figures 2-3 illustrate the effects of impedance $\left(\bar{\lambda}\right)$ with stenosis height (δ_1) for different values of couple stress fluid constraints $\left(\bar{\alpha},\eta\right)$ and thermophoresis and Brownian motion constraints (N_t,N_b), respectively. In Fig.2, couple stress fluid constraints are considered as $\bar{\alpha} = 0.1,0.5,0.9$ and $\eta = 0.4, 0.6, 0.8$ for curves 1-6, respectively. Similarly, curves 1-6 in Fig. 3 are plotted for a fixed value of $N_b = 0.1,0.5,0.9$ and $N_t = 1.0, 2.0, 3.0$, respectively. It is noticed from both the figures that the skin-friction or impedance $\left(\bar{\lambda}\right)$ increases with the size of the stenosis height (δ_1). It is also noticed that the increasing value of the Brownian motion (N_b), thermophoresis (N_t) and couple stress fluid constraints $\left(\bar{\alpha},\eta\right)$, affect Strongly the skin-friction.

Figures 4-5 show the impacts of impedance $\left(\bar{\lambda}\right)$ with respect to dilatation height (δ_2). The curves in these figures have been plotted under the same assumption as in the preceding figures (Figs 2-3). It is found that the nature of the impedance is completely opposite, i.e., skin-friction or impedance is reduced with the increase of dilatation height. Further, it is observed that impedance $\left(\bar{\lambda}\right)$ curves increases with the increase of couple stress fluid constraints $\left(\bar{\alpha},\eta\right)$ and thermophoresis constraint N_t, but the impedance curves decreases with the increase of the Brownian motion constraint (N_b). This means that the presence of stenosis or dilatation in the artery will not change the effect of the Brownian motion on impedance.

Figures 6-8 depict the validation of the wall shear stress (τ_h) against stenosis height (δ_1). The shear stresses along the wall have been presented in Figs. 6-8 for different values of couple stress fluid constraints $\left(\bar{\alpha},\eta\right)$, and local temperature (G_r) and nanoparticle concentration (B_r); and Brownian motion (N_b) and thermophoresis (N_t) parameters, respectively. The different values of the above parameters used to plot the figures are mentioned inside the figures. The wall shear stress (τ_h) grows with the increasing values of stenosis δ_1. It can also be noticed that the wall shear stress (τ_h) curves decrease with the increase of couple stress fluid constraints $\left(\bar{\alpha},\eta\right)$ and Brownian motion (N_b) and curves are increased with the increasing value of thermophoresis (N_t), local temperature (G_r) and nanoparticle concentration (B_r). Similarly, the wall shear stress (τ_h) is acting over the height of the dilatation (δ_2) as shown in Figs 9-11. It is also noticed that the wall shear stress grows with the rising values of N_t, G_r and B_r but it decreases with decreasing values of dilatation $\delta_2, \bar{\alpha},\eta$ and N_b.
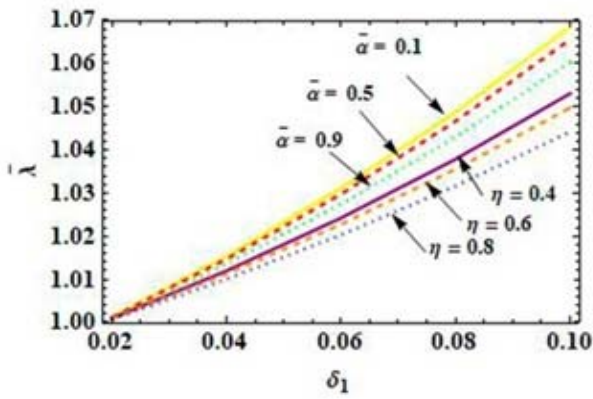
Fig.2. Sketch of δ_1 and $\bar{\alpha}, \eta$ on $\bar{\lambda}$ with $d_1 = d_2 = 0.2, L_1 = 0.2 = L_2, L = 1, q = 0.1$.
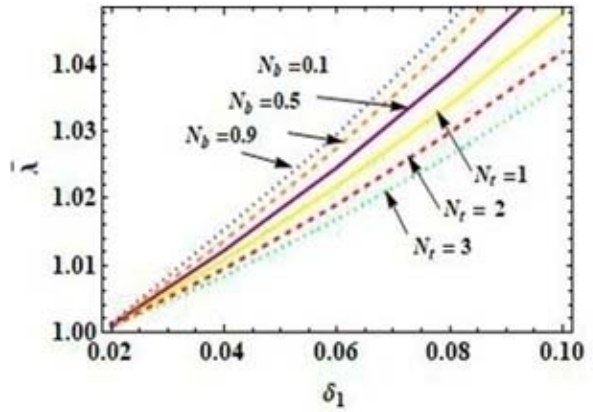
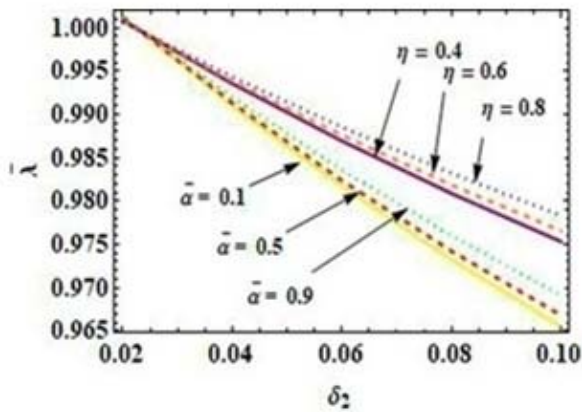Fig.3. Sketch of δ_1 and N_b, N_t on $\bar{\lambda}$ with $d_1 = d_2 = 0.2, L_1 = 0.2 = L_2, L = 1, q = 0.1$.

Fig.4. Sketch of δ_2 and $\bar{\alpha}, \eta$ with $d_1 = d_2 = 0.2, L_1 = 0.2 = L_2, L = 1, q = 0.1$.
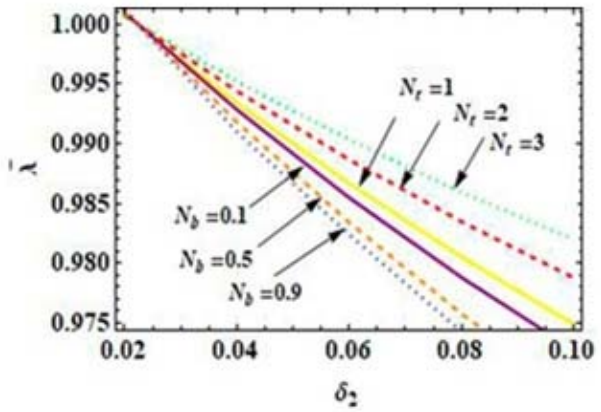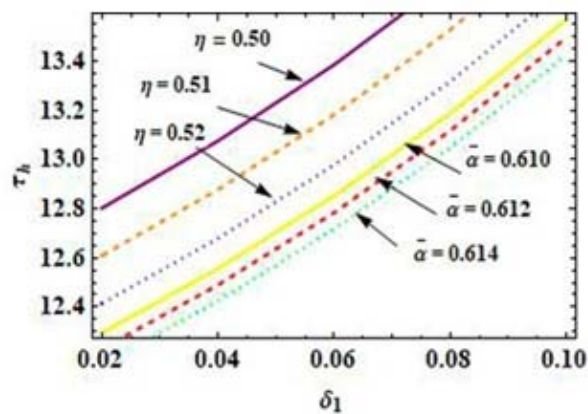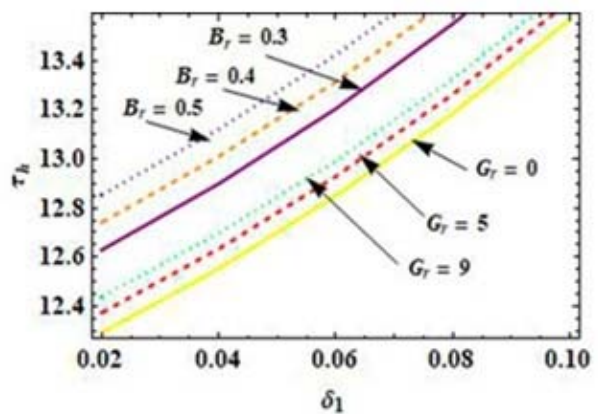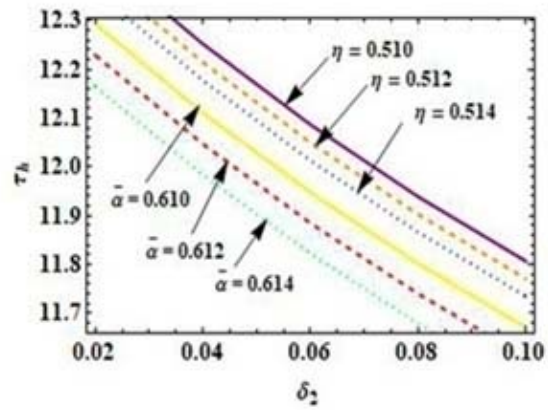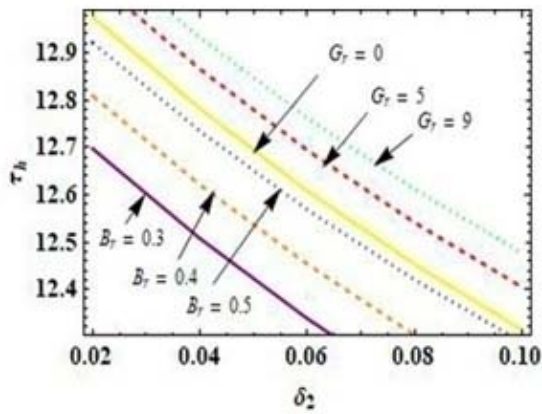
Fig.5. Sketch of δ_2 and N_b, N_t on $\bar{\lambda}$ with $d_1 = d_2 = 0.2, L_1 = 0.2 = L_2, L = 1, q = 0.1$.

Fig.6. Sketch of δ_1 and $\bar{\alpha}, \eta$ on τ_h with $d_1 = d_2 = 0.2, L_1 = 0.2 = L_2, L = 1, q = 0.1$.

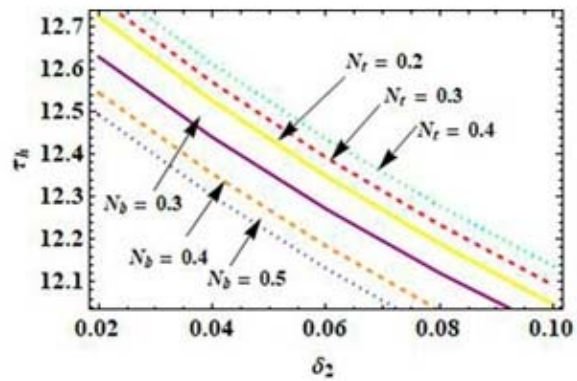Fig.7. Sketch of δ_1 and B_r, G_r on τ_h with $d_1 = d_2 = 0.2, L_1 = 0.2 = L_2, L = 1, q = 0.1$.
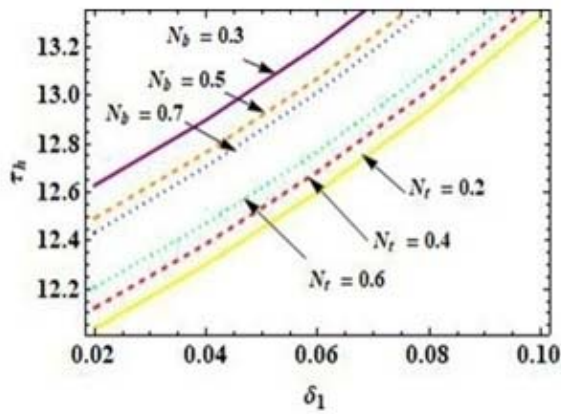
Fig.8. Sketch of δ_1 and N_b, N_t on τ_h with $d_1 = d_2 = 0.2, L_1 = 0.2 = L_2, L = 1, q = 0.1$

Fig.9. Sketch of δ_2 and $\bar{\alpha}, \eta$ on τ_h with $d_1 = d_2 = 0.2, L_1 = 0.2 = L_2, L = 1, q = 0.1.$

Fig.10. Sketch of δ_2 and B_r, G_r on τ_h with $d_1 = d_2 = 0.2, L_1 = 0.2 = L_2, L = 1, q = 0.1$

Fig.11. Sketch of δ_2 and N_b, N_t on τ_h with $d_1 = d_2 = 0.2, L_1 = 0.2 = L_2, L = 1, q = 0.1.$

The development of an inside circulating bolus of liquid (by closed streamlines) is called trapping/catching and this trapped/caught bolus is pushed ahead beside the peristaltic wave. To get more insight into the flow behavior, the geometric contours, Figs 12-19, are intended to illustrate the blood flow pattern at the diseased segment. Figures 12(a-c) and Figs. 13(a-c) show the impact of couple stress liquid constraint on the flow profile. As the couple stress constraint expands, the flow lessens at the stenosis segment and ascends at the post stenotic dilation segment, which makes the bolus shrink and enlarge respectively. In the same way, the influence of different constraints on catching/tapping is shown in Figs 14-19. It is observed that the size of caught/trapped bolus enlarges with growths in δ_1, N_t while the size of the bolus shrinks with N_b, G_r, B_r and $\delta_2.$
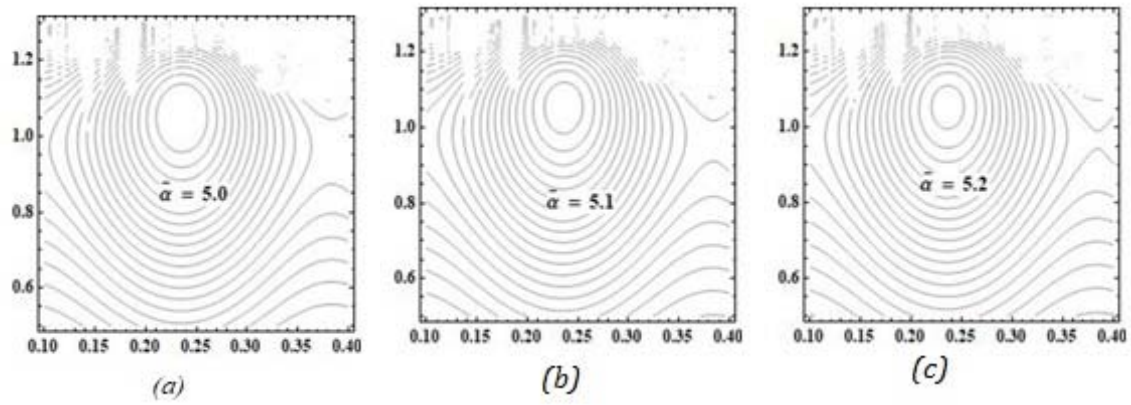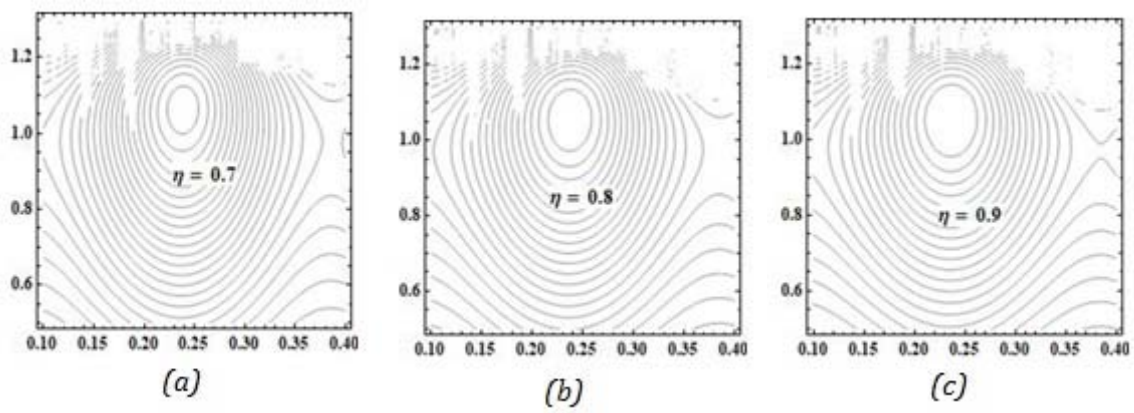
Fig.12. Flow line patterns for $\overline{\alpha}$.

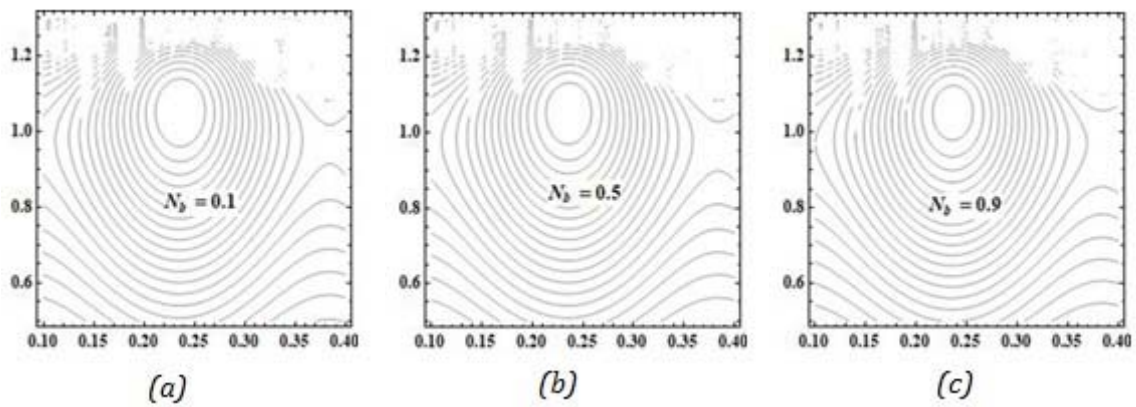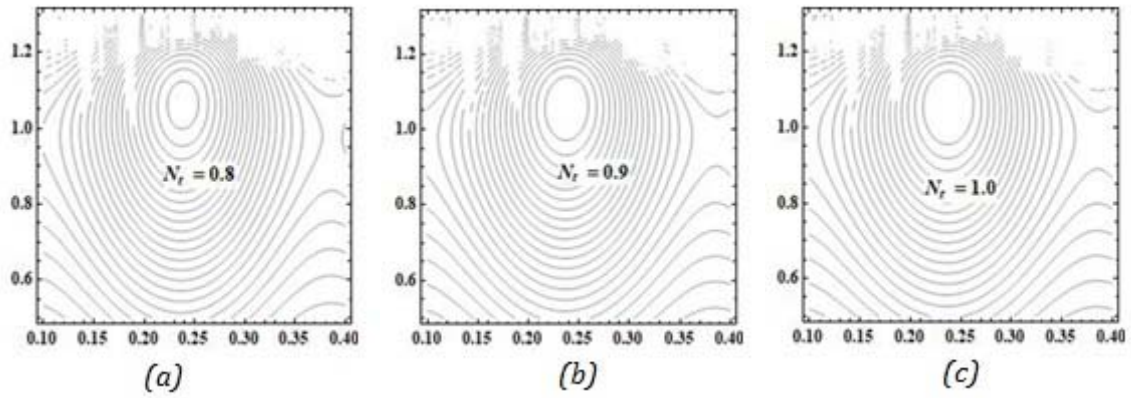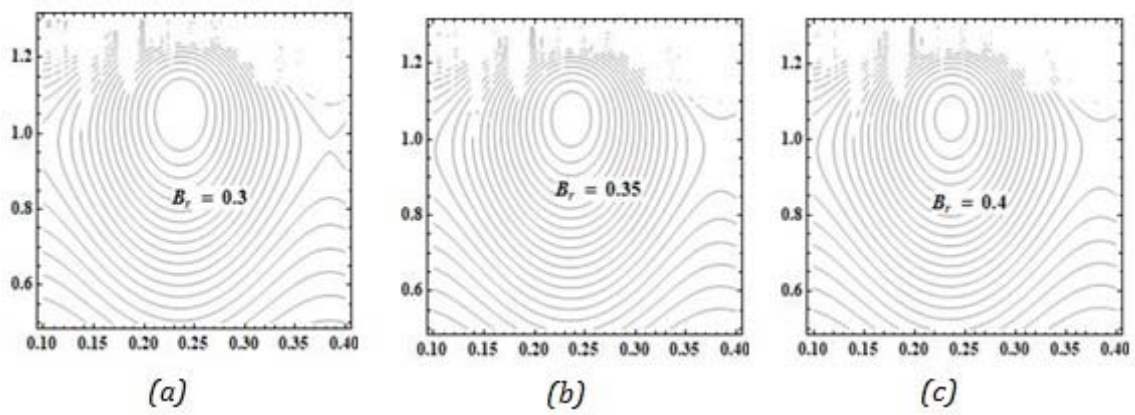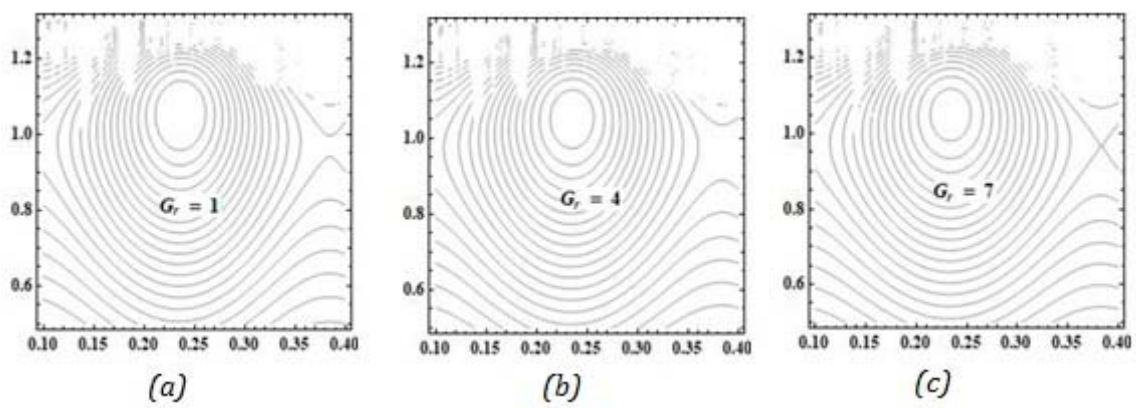Fig.13. Flowline patterns for η.

Fig.14. Flow line patterns for N_b .

Fig.15. Flow line patterns for N_t.

Fig.16. Flow line patterns for B_r.

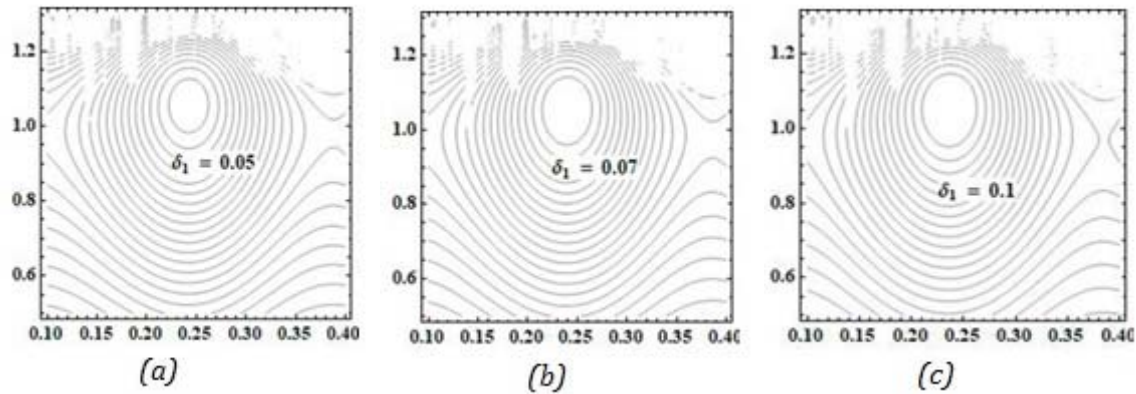Fig.17. Flow line patterns for G_r.
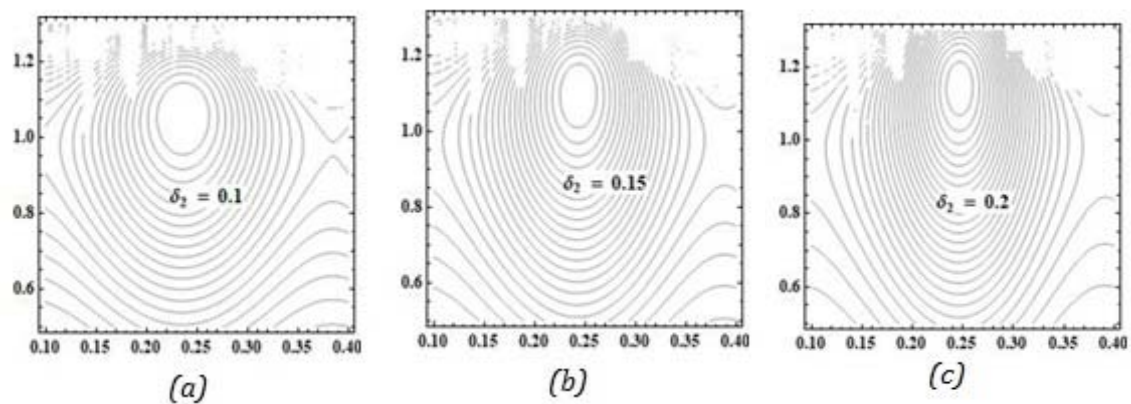
Fig.18. Flow line patterns for δ_1.

Fig.19. Flow line patterns for δ_2.

4. Concluding remarks

A mathematical model of a steady and incompressible couple-stress fluid with nanoparticles in a tube having stenosis and post stenotic dilation is analyzed. Using the homotopy perturbation method with appropriate boundary conditions, analytical relations for impedance and wall shear stress have been computed. The phenomena of nanoparticle concentration and heat transfer have been investigated an account of their importance in the rheology of blood. The couple stress fluid is used to depict the behavior of blood flow. The obtained results are presented graphically for different values of couple stress, thermophoresis, Brownian motion constraints, dilatation, stenosis, local temperature, and nanoparticle concentration. The study shows that resistance to the flow and impedance are maximum at the neck of dilatation height and minimum at the neck of stenosis. The results have been obtained for low to high values of stenosis and dilatation height parameters.

Nomenclature

B_r − nanoparticle concentration

Gr − local temperature

L_i − i^{th} diseased section length

N_b − Brownian constant

N_t − thermophoresis constraint

q − volume flow rate

R − tube radius at dilatation

R_0 − tube radius of the normal segment

r − radial distance

u − velocity of the fluid

α_i − first i^{th} diseased segment distance from the origin

$\overline{\alpha}, \eta$ − couple stress fluid constraints

β_i − i^{th} abnormal segment distance from the origin

Δp − pressure drop over one wavelength

δ_i − i^{th} abnormal section

δ_1, δ_2 − height of the stenosis

θ_t − temperature of the fluid

λ − resistance to flow

τ_h − wall shear stress

References

[1] Young D.F. (1968): *Effect of a time-dependent stenosis on flow through a t*ube.– Trans. ASME J. Engng. Ind., vol.90, pp.248-254.

[2] Misra J.C., Patra M. K. and Misra S.C. (1993): *A non-Newtonian fluid model for blood flow through arteries under stenotic conditions.–* J. Biomech., vol.26, No.9, pp.1129-1141.

[3] El-Shahed H.M. (2003): *Pulsatile flow of blood through a stenosed porous medium under periodic body acceleration.–* Appl. Math. Comput. vol.138, pp.479-488.

[4] Mandal P. K. (2005): *An unsteady analysis of non-Newtonian blood flow through tapered arteries with a stenosis.–* Int. J. Nonlin. Mech., vol.40, pp.151-164.

[5] Misra J.C. and Shit G.C. (2006): *Blood flow through arteries in a pathological state: A theoretical study.–* Int. J. Eng. Sci., vol.44, pp.662-671.

[6] Ramana J.V.R., Srikanth D., Samir D. and Das K. (2017): *Modelling and simulation of temperature and concentration dispersion in a couple stress nanofluid flow through stenotic tapered arteries.–* Eur. Phys. J. Plus., vol.132, No.8, pp.365.

[7] Nadeem S., Ijaz S. and Akbar N.S. (2013): *Nanoparticle analysis for blood flow of Prandtl fluid model with stenosis.–* Int. Nano Lett., vol.3, pp.35.

[8] Prasad K.M., Subadra N. and Reddy S.K. (2017): *Peristaltic transport of a couple stress fluid with nanoparticles having permeable walls.–* J. Nanofluids., vol.6, pp.751-760.

[9] Jyotirmoy R. and Murthy P.V.S.N. (2016): *Unsteady solute dispersion in non-Newtonian fluid flow in a tube with wall absorption.–* Phil. Trans. R. Soc. A. Math. Phys. Eng. Sci., vol.472 No.2193, pp.20160294.

[10] Elnaqeeb T., Mekheimer K.S. and Alghamdi F. (2016): *Cu-blood flow model through a catheterized mild stenotic artery with a thrombosis.–* Math. Biosci., vol.282, pp.135-146.

[11] Valanis K. C. and Sun C. T. (1969): *Poiseuille flow of a fluid with couple stress with applications to blood flow.–* J. Biorheol., vol.6, No.2, pp.85-97.

[12] Srinivasacharya D. and Srikanth D. (2008): *Effect of couple stresses on the flow in a constricted annulus.–* Arch. Appl. Mech., vol.78, No.4, pp.251-257.

[13] Ponalagusamy R. (2017): *Two-fluid model for blood flow through a tapered arterial stenosis: effect of non-zero couple stress boundary condition at the interface.–* Int. J. Appl. Comput. Math., vol.3, pp.807-824.

[14] Reddy J.V.R., Srikanth D. and Murthy S.K. (2014): *Mathematical modelling of couple stresses on fluid flow in constricted tapered artery in presence of slip velocity-effects of catheter.–* Appl. Math. Mech., vol.35, No.8, pp.947-958.

[15] Wang P., Li Z., Wu X. and An Y. (2015): *Taylor dispersion in a packed pipe with wall reaction: based on the method of Gill's series solution.*– Int. J. Heat Mass Transfer, vol.91, No.12, pp.89-97.

[16] Liao S. (2003): *Beyond Perturbation: Introduction to the Homotopy Analysis Method.*– Chapman and Hall/CRC, New York.

[17] He J. H. (2000): *Variational iteration method for autonomous ordinary differential systems.*–Appl. Math. Comput., vol.114, No.2, pp.115-123.

[18] He J. H. (2004): *Comparison of homotopy perturbation method and homotopy analysis method.*– Appl. Math. Comput. vol.156, No.2, pp.527-539.

[19] Rahbari A., Fakour M., Hamzehnezhad A., Vakilabadi M.A. nad Ganji D.D. (2017): *Heat transfer and fluid flow of blood with nanoparticles through porous vessels in a magnetic field: A quasi-one-dimensional analytical approach.*– Math. Biosc., vol.283, pp.38-47.

[20] Batchelor G. K. (1977): *The effect of Brownian motion on the bulk stress in a suspension of spherical particles.*– J. Fluid Mech., vol.83, No.1, pp.97-117.

[21] Hatami M., Hatami J. and Ganji D.D. (2014): *Computer simulation of MHD blood conveying gold nanoparticles as a third grade non-Newtonian nanofluid in a hollow porous vessel.*– Comput. Meth. Prog. Bio., vol.113, No.2, pp.632-641.

[22] Nadeem S. and Ijaz S. (2014): *Nanoparticles analysis on the blood flow through a tapered catheterized elastic artery with overlapping stenosis.*– Eur. Phys. J. Plus., vol.129, No.11, pp.249.

[23] Reddy J.V.R. and Srikanth D. (2020): *Impact of blood vessels wall flexibility on the temperature and concentration dispersion.*– J. Appl. Comput. Mech., vol.6, No.3, pp.564-581.

[24] Pincombe B., Mazumdar J. and Hamilton-Craig I. (1999): *Effects of multiple stenoses and post-stenotic dilation on non-Newtonian blood flow in small arteries.*– Med. Biol. Eng. Comput., vol.137, pp.595-599.